# Integrating Cross-Layer LTE Resources and Energy Management for Increased Powering of Base Stations From Renewable Energy

Andres Kwasinski[1] and Alexis Kwasinski[2]
[1]Department of Computer Engineering, Rochester Institute of Technology, USA, andres.kwasinski@rit.edu
[2]Department of Electrical and Computer Engineering, University of Pittsburgh, USA, akwasins@pitt.edu.

***Abstract*— This paper studies a cross-layer technique to increase the powering of an LTE macro base station from renewable energy. The cross-layer technique integrates the management of the transmit antennas and LTE frames with, at the application layer, video compression factor and data traffic delay. Importantly, the management of these cellular network components is integrated with the base station energy system by adapting the transmission of the cellular network based on the projected renewable energy availability. The overall system presents a tradeoff between increased use of renewable energy and an increase in video distortion and data delay up to predefined limits. Simulation results show that the studied technique effectively increases the percentage of time that an LTE base station is able to operate powered only from renewable energy (up to 98.5%) while at the same time increasing within small, acceptable levels, video distortion and data delay a third of the time.**

## I. Introduction

Information and Communications Technology (ICT) infrastructure currently accounts for 2% of the global carbon footprint which is a share equivalent to that of the airline industry, [1]. Moreover, in developed countries this impact may be as high as 10% and is expected to grow yearly by 4% until 2020, [2]. When accounting for the very rapid growth of cellular networks infrastructure, it is key to investigate technologies to reduce the use of non-renewable energy. In this regard, cellular network operators focus their attention on the base stations because they account for more than half of their energy expenditure [3]. One way to reduce the carbon footprint of cellular base stations is to reduce their power consumption. For this, some of the techniques that have been recently investigated are dynamic scheduling, optimization of cell deployment and improving RF power amplifiers' efficiency (as discussed in [4] and references therein), turning off selected base stations when the network is lightly loaded, [5], [6], using cell site cooperation [7], coverage/spectrum optimization and interference mitigation (e.g., through femtocells [8]), and resource allocation for a given traffic condition in the network, as in [9], [10], [11], [12].

Since powering base stations from the main electric grid usually implies the use of energy from fossil fuels, it is justifiable to consider powering them as much as possible from renewable sources of energy (e.g. solar or wind energy). The use of renewable sources of energy to power cellular base stations also has the benefits of providing the means to power a base station in situations where the grid is not accessible (e.g. in remote rural areas or when natural events disrupt the working of the grid). Among different works that consider the use of renewable sources of energy in cellular networks, [13] considered the design of the power generation and storage subsystems, [14] studied a system where multiple base stations cooperate in redistributing available energy and [15] studied base station sleeping control and resource allocation when powering from renewable sources.

All the works cited so far take cellular traffic conditions and QoE requirements as given and not subject to external control. In [16], we indicated that it is possible to switch off one base station, and extend the use of renewable energy, at any traffic load by shaping the traffic so that conversational traffic quality was slightly reduced and data delay increased. In [17] we build upon this idea and introduced a mechanism that adapts the power consumption of LTE base stations (called "eNBs") by managing the volume of cellular traffic that is serviced based on the short term availability of renewable energy. Our approach differs from all other works by treating traffic conditions and Quality-of-Experience (QoE) requirements as controllable nobs. In [17], the end-user QoE and the power consumed by the base station (and, consequently, the percentage of time that the eNB can be powered from renewable sources) are linked through the number of resource blocks (in LTE, a resource block -RB- is the minimum unit of time-frequency resource allocation and is composed by an array of 12 subcarriers by 7 OFDM symbols). This allowed for the development of an integrated energy-cellular traffic management technique that adapts to a predicted reduction in available renewable energy by shaping the traffic through a controlled, smooth and transient reduction of real-time video quality and increase in data delay. While not studying the specific problem hereafter, it is still worth mentioning the works [18] and [19] that considered techniques with integrated energy harvesting and wireless transmission management.

In this paper we continue work on our novel approach that trades off the users' QoE with longer operation from renewable sources. The overarching goal for the techniques that we study herein is to reduce as much as possible the probability that the state of charge (SoC) of the batteries used to store renewable energy at the eNB is below a deep discharge threshold, while reducing as little as possible the users' QoE. Because they account for almost all the cellular traffic through the eNB [28],

This material is based upon work supported by the National Science Foundation under awards No. CCF-1331788 and ECCS-0845828.

978-3-9018-8273-9/15/ ©2015 IFIP

in this work we consider real-time video sessions, with the user QoE measured in peak signal-to-noise ratio (PSNR), and data traffic, with the user QoE measured as relative increase in delay. This approach effectively introduces an extra design dimension that allows for the management of the energy used by an eNB for all traffic conditions (different from other works that manage the energy used only when allowed by low traffic conditions). While in [17] we studied traffic shaping based on controlling only the number of active resource blocks, we consider now traffic shaping that is controlled by changing both the number of transmit antennas and resource blocks. For this, our novel contribution here is first to show that the best approach to meet the stated goals is by shaping traffic primarily through controlling the number of transmit antennas and secondarily through managing the number of RBs used. In addition, in this paper we contribute an optimal solution to the derived problem of distributing a given number of resource blocks between a combination of video and data calls so that the overall QoE is maximized.

Results obtained using actual solar and wind energy measurements and a detailed LTE network simulation will show that the presented traffic shaping technique clearly improves our results from [17], reducing the probability of not being able to power the eNB from renewable energy more than ten times (from 20% to 1.5%) and reduces seven times the probability of operating into a deep discharge cycle the battery bank that stores renewable energy at the eNB. The results also show how the presented technique allows to control the tradeoff between the probability of powering from renewable energy and the video quality reduction and data delay increase. Indeed, with the proposed technique, video quality is reduced only a third of the time and by more than 3 dB only 2% of the time and data delay is increased only 29% of the time.

The rest of this paper is organized as follows. In Section II we describe the system setup, and we present a traffic shaping technique to increase renewable energy use at the eNB in Section III. Section IV discusses performance evaluation results. Concluding remarks are given in Section V.

## II. System Setup

In this work we will study the powering of an LTE eNB using renewable sources of energy, primarily from photovoltaic (PV) panels and wind turbines. Wind turbines could be with a horizontal axis, which tend to be more efficient but have a larger footprint. Because of its size, a horizontal axis turbine would be normally shared by multiple eNBs. Nonetheless, horizontal axis wind turbines may have a height similar to many cell site antenna towers. If for a residential suburban location it is desired to have smaller wind turbines at each cell site, a typical setup would use a vertical axis turbine. Such a turbine may have a maximum power output of 10 kW with a diameter of 6 m. and pillar height of 5.5 m. The power that can be obtained from a solar panel is directly proportional to its area. In this work we will consider data obtained from an array of 26 MX Solar USA Suncase MX60-240 panels installed at the Rochester Institute of Technology's

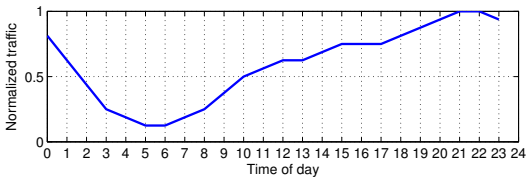


Fig. 1. Normalized average data traffic profile in Europe, from [22].

Golisano Institute for Sustainability. Each panel has a size of 1.7 $m^2$ and is capable of generating a maximum of 240 W. These are typical values for current technology. The use of electric generators located near or at the eNB sites, instead of drawing renewable energy from the main grid, is advantageous because it enables the integrated management of traffic shaping and base station energy subsystem. Also, the use of electric generators located near or at the eNB sites increases the resiliency of the cellular communication infrastructure by avoiding the weaknesses associated with long electric power distribution lines.

There are two main challenges related to the use of renewable sources of energy. The first challenge is physical footprint; obtaining large values of energy from renewable sources require infrastructure setups that occupy a large physical area. The second main challenge related to the use of renewable source of energy is their variability. Both solar and wind energy availability changes with the weather and, of course, solar energy is unavailable during nighttime. This variability is firstly addressed through the use of a battery bank that stores renewable energy when it is available in excess to be used at a later time when there is a deficit in available renewable energy. As it turns out, the cost associated with battery banks is one of the main factors limiting the growth of renewable energy applications. This is not an issue in our case because we leverage the battery banks that are already present at eNB sites for use as a backup source of energy when there is a failure in the grid power supply. Indeed, cell sites are often equipped with battery banks that are used to power the base station in case of a power outage. In their typical use, the battery banks present a financial dilemma to cellular operators because they are of critical need but used sparsely. Our setup leverages the battery bank infrastructure already in place and uses it continuously. As such, we assume that the energy that is obtained from the PV panels and wind turbines is used to charge the battery bank and the eNB draws the energy to operate from the battery bank. Therefore, when the battery bank is completely discharged means that the eNB cannot be powered from renewable energy at that time and power that is likely from fossil fuels needs to be drawn from the main electric grid. Another technique that is used to absorb the variability of renewable energy relies on diversifying the sources by using more than one renewable energy type, which in our case takes the form of using wind and sun energy.

For the cellular infrastructure, we will assume that each of the eNB to be considered herein are typical for an LTE network in an urban environment. Each eNB is a macro base station, servicing three sectors operating with an assumed two transmit and two received MIMO configuration, transmitting

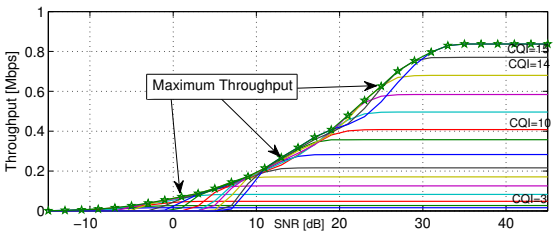


Fig. 2. Throughput for each CQI and maximum throughput adaptive selection per RB in a 2x2 MIMO LTE system under a Vehicular A channel.

at a power of 40 dBm and assumed to be separated 500 m from the closest eNBs (as assumed in the study [22]). Without loss of generality, the LTE system was assumed to be FDD with a 10 MHz bandwidth and frequency reuse factor 3.

The received signal power, $P_{Rx}$ undergoes path, penetration and shadowing loss, and, at a distance $d$ km between eNBs, it is $P_{Rx} = P_{Tx} - 128.1 - 37.6 \log d - 10 - S$, [22], where all magnitudes are in dBs, $P_{Tx}$ is the transmit power, $S$ is the shadowing loss (modeled as a zero-mean Gaussian random variable with 8 dB standard deviation) and the penetration loss is fixed at 10 dB. In addition, delay spread for all channels is modeled as being with equal probability either the Pedestrian B or the Vehicular A typical urban model from [23] . Also, LTE implements adaptive modulation and coding (AMC), where the channel signal-to-interference-plus-noise ratio (SINR) is mapped to a Channel Quality Indication (CQI) number (between 1 and 15), which is in turn mapped to a combination of modulation mode (QPSK, 16-QAM and 64-QAM) and channel coding rate (several options). For any given SINR,

$$\beta = \frac{P_{Rx}}{\sum_{i \in I} P_{I_i} + N_0},$$

where $P_{I_i}$ is the received power from the interfering eNB $i$ in the set $I$, and $N_0$ is the background noise (assumed with a power spectral density of -174 dBm/Hz), there is a combination of modulation mode and channel coding rate that results in the maximum throughput per Resource Block (RB). Figure 2 shows, per RB, the throughput obtained for each CQI, and the AMC maximum throughput obtained in the considered LTE system with a 2x2 MIMO configuration and a maximum of 3 layer-2 retransmissions allowed. The results were obtained using the LTE simulator from the TU Wien, [24].

From the viewpoint of the electric power subsystem, the eNB is an externally controllable load. We modeled the electric load from the eNB following [22]. According to this model, the load can be separated into a constant component and a dynamic component. The constant consumed power, equal to 65 W per transmitter unit in our model, accounts for the radio resource overhead (e.g. for pilot signals), cooling, processing, baseband interface, etc. In an LTE system, the dynamic power consumption component changes according to the intensity of cellular traffic through the eNB, increasing practically in a linear fashion following the fraction of the total resource blocks (RBs) in a frame that are active in the transmission of cellular traffic. In the sequel we will denote this fraction as $R_B[k]/R_B^{(T)}$, where $R_B^{(T)}$ is the total number of RB in an LTE frame and $R_B[k]$ is the number of those that are used in the frame transmission. As stated earlier, the energy stored at the battery bank at some time $n$, $S[n]$, will equal the previous evolution over time of the difference between the energy that is obtained from renewable sources and the energy that is drawn by the eNB. Then, this relation can be written as,

$$S[n] = S[0] + T \sum_{k=1}^{n} \left( \xi[k] - N[k](97\nu[k] \frac{R_B[k]}{R_B^{(T)}} + 65) \right), \quad (1)$$

where $T$ is the duration of one traffic shaping control time period (taken without loss of generality equal to 1 hour), $\nu[k]$ is the traffic profile at time $k$, as shown in Fig. 1, normalized to the maximum traffic intensity, $S[0]$ is the initial battery charge and $T\xi[k]$ is the energy provided by renewable sources during the $k$th. time period. In order to keep notation simple, (1) is not including the limits on $S[n]$, $0 \leq S[n] \leq B$, $\forall n \geq 0$, where $B$ is the battery bank energy storage capacity. In (1), $N[k]$ is the number of active radio transmitters at the eNB at time $k$ and it equals the number of serviced sectors times the number of transmit antennas for each sector.

Our present goal is to increase as much as possible the time that an eNB is powered from renewable sources of energy while reducing as little as possible the users' QoE. In our previous work, [17], we formulated the goal of increasing as much as possible the time that an eNB is powered from renewable sources of energy as reducing the probability that the battery bank would be completely discharged. In this work we change the formulation for this goal to also consider that deep discharge cycles for the battery bank are the main factor in reducing their lifetime. Consequently, our goal for the battery bank will to avoid as much as possible for the battery SoC, $S[n]/B$ to go below a threshold for a deep discharge. A typical value for this threshold is between 0.2 and 0.3. To meet this goal, the power that is consumed by the eNB will be adapted accordingly. Based on (1), we propose to manage the power consumed by the eNB by reducing the number of transmit antennas, which affects the value for $N[k]$, and the number of active RBs, $R_B[k]$. Note that $N[k]$ could be changed not only by changing the number of transmit antennas but also when setting a base station or a sector into sleep mode. In our case, we will change the number of transmit antennas but we will not set to sleep a sector or the base station (i.e. for the assumed setup, the possible choices for $N[k]$ are 6, 5, 4 and 3). As mentioned, the approaches of setting a base station or a sector into sleep mode have been studied elsewhere and are not the focus of this work. Yet, this point conveys the observation that the technique that will be presented in this paper can be used concurrently with other techniques in the literature. Also, note that reducing the number of active resource blocks, reduces the volume of cellular traffic that is carried by the eNB. Similarly, as illustrated in figure 3 when reducing the number of transmit antennas from two to one also results in (in ideal settings) halving the throughput associated with a RB. As a result, managing the power consumed by the eNB could reduce the throughput for the active transmissions and, consequently, reduce the QoE for the users. Because of this, the proposed technique increases the time that the eNB

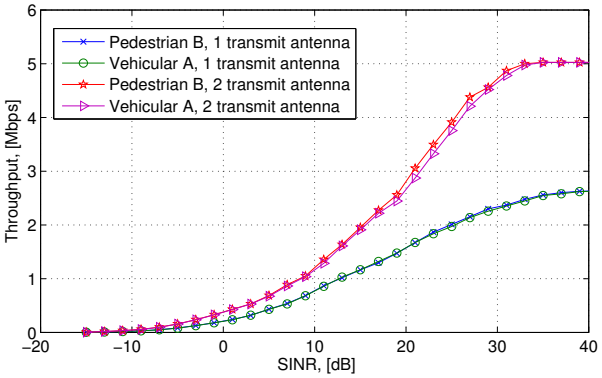


Fig. 3. Maximum throughput per RB in a Vehicular A and Pedestrian B channels with one and two transmit antennas.

is powered from renewable energy by managing the power consumed through traffic shaping. The technique effectively establishes a tradeoff between the increase in powering from renewable energy and the reduction in users' QoE.

It will be assumed that most of the traffic is composed of real-time/streaming video and regular data because they effectively account for almost all the cellular traffic through the base station [28] (video, in fact, accounts for more than 50 % of all the traffic load). Voice traffic, even if wideband, accounts for a very small portion of all traffic and, if needed, could be considered as a negligible portion of the real-time traffic. The video QoE will be measured in terms of the peak signal-to-noise ratio (PSNR) and data sessions QoE will be measured in terms of the increase in delay relative to the case when no traffic shaping is implemented. Traffic shaping will increase the compression ratio of video and reduce the transmit rate for data traffic. Real time video compression ratio can be controlled without adding any delay or jitter by leveraging the scalability features found in modern video codecs. In shaping the traffic, the goal is to smoothly reduce the service provided by the eNB in a controlled way, so impact to the users (reduced video quality and increased data delay) remains acceptable and little noticeable.

## III. Number of Transmit Antennas and Resource Blocks Management

We first address the question of whether, for our stated goals, it is better to manage power consumption at the eNB by changing the number of transmit antennas or by changing the number of active resource blocks. The following three remarks answer this question:

*Remark 1*: The same relative change in $N[k]$ and $R_B[k]/R_B^{(T)}$ results in a larger variation in power consumed from the change in $N[k]$. This remark can be seen by following a sensitivity analysis. To simplify notation, we first introduce $\pi[k] = R_B[k]/R_B^{(T)}$. Next, consider the change in battery SoC, $\Delta S_N$, that results from a relative change $\delta_N$ in $N[k]$,

$$\Delta S_N = T\delta_N N[k](97\nu[k]\pi[k] + 65),$$

and the change in battery SoC, $\Delta S_\pi$, that results from a relative change $\delta_\pi$ in $\pi[k]$,

$$\Delta S_\pi = TN[k]97\nu[k]\delta_\pi\pi[k].$$

It is now straightforward to see that for $\delta_N = \delta_B$, $\Delta S_N - \Delta S_\pi = 65T\delta_N N[k] > 0$, or $\Delta S_N > \Delta S_\pi$.

*Remark 2*: It is well-known that both video distortion and data traffic delay are monotonically reduced when increasing the transmit bit rate.

*Remark 3*: While keeping all other variables unchanged, the transmit bit rate per RB changes with the same ratio for equal relative changes in the number of transmit antennas and the number of resource blocks. This is, if we reduce the number of transmit antennas in a sector from two to one, the transmit bit rate per RB will be halved, just us the same will happen if we halved the number of active resource blocks (i.e. if we make $\pi[k] = 0.5$).

Following these remarks, changing $N[k]$ and $R_B[k]$ so that $\Delta S_N = \Delta S_\pi$ would be achieved with $\delta_N < \delta_\pi$, which would translate in a smaller reduction in the users' QoE when changing $N[k]$ compared to changing $R_B[k]$. In conclusion, for our stated goals, it is better to manage power consumption at the eNB by changing the number of transmit antennas first because $N[k]$ is more effective in changing power while reducing the users' QoE the least.

Having answered the first design question, we next address the question of determining $N[n+1]$ for the next control period to avoid as much as possible for the battery state of charge (SoC), $S[n]/B$, to go below a threshold corresponding to a deep discharge cycle. This threshold will be denoted as $L$. In the proposed technique, $N[k+1]$ is obtained by determining a target value for the energy stored in the battery bank $S_T[n+1] = \hat{S}[n+1] + S_D$, where $\hat{S}[n+1]$ is the predicted value for the energy stored in the battery bank at time $n+1$ (the next decision time) and $S_D$ is the difference in energy drawn from the batteries so as to meet the target $S_T[n+1]$. The predicted value $\hat{S}[n+1]$ is calculated from estimates for traffic load, $\hat{\nu}[n+1]$, and renewable energy availability, $\hat{\xi}[n+1]$, and with the assumption that no traffic shaping is done (i.e. $N[n+1]$ equals its maximum value $N_F$ and $R_B[n=1] = R_B^{(T)}$). Due to space constrains, the estimation of traffic load and renewable energy availability exceeds the scope of this work and will be assumed to be ideal. From its definition, determining $S_T[n+1]$ implies finding $S_D$. Based on the goal to prevent the battery SoC to reach deep discharge values we have that,

$$S_D = \max\left\{0; (LB - \hat{S}[k]), k = n+1, \ldots, n+M\right\}, \quad (2)$$

because, with all other variables staying unchanged, setting $S_T[n+1] = \hat{S}[n+1] + S_D$ will make the signal $S[k]$ for $k = n+1, n+2, \ldots, n+M$ be shifted to values $S[k] + S_D \geq LB$. In (2), $\hat{S}[k]$ is the predicted value for the energy stored in the battery bank at time $k$ (obtained in identical way as $\hat{S}[n+1]$).

Based on the value for $S_D$ from (2), $N[n+1]$ is calculated using (1) with $R_B[k] = R_B^{(T)}$ (only the number of transmit antennas is changed) and by considering that from its definition $S_T[n+1] = S_D + S[n] + T(\hat{\xi}[n+1] - N_F(97\hat{\nu}[n+1] + 65))$. At the same time, the application of traffic shaping at time $n+1$ will result in the energy stored in the batteries to be $S_T[n+1] = S[n] + T(\hat{\xi}[n+1] - N[n+1](97\hat{\nu}[n+1] + 65))$.

Equating the two expressions for $S_T[n+1]$ and operating, results in

$$N[n+1] = \left\lceil N_F - \frac{S_D}{97\hat{\nu}[n+1]+65} \right\rceil, \quad (3)$$

where $\lceil \cdot \rceil$ denotes the ceiling operation, which was chosen (instead of rounding or the floor operation) to match the goal of affecting the users' QoE as little as possible. At the same time $N[n+1]$ can take values only from the set $\{N_F = 6, 5, 4, 3\}$. Values larger than 6 are not possible because there are no more radio transmitters at the eNB and values less than 3 would mean that at least one sector is set in sleep mode (a case that is not studied in this paper). A value for $N[n+1]$ equal to 5 or 4 indicates that transmission in some sectors is done with two antennas and with one antenna in the rest. Because of the limited number of choices for the values that $N[n+1]$ could take, the actual energy stored in the batteries at time $n+1$ will likely be less than the target $S_T[n+1]$, indicating a power consumption larger than the target. In our proposed technique, $R_B[n+1]$ is adjusted to provide the finer adjustment on the power consumption. We limit the changes to $R_B[n+1]$ only to those sectors operating with two transmit antennas (because the idea of adjusting $R_B[n+1]$ is to compensate for the effects of the ceiling operation in (3)). Let $N_2$ and $N_1$ be the number of sectors operating with two and one transmit antennas respectively. When traffic shaping also changes $R_B[n+1]$ for the sectors with two active transmit antennas, we have $S_T[n+1] = S_D + S[n] + T(\hat{\xi}[n+1] - N_1(97\hat{\nu}[n+1]+65) - 2N_2(97\hat{\nu}[n+1]R_B[n+1]/R_B^{(T)}+65))$. Operating in form analogous to the derivation of (3), we get

$$R_B[n+1] = \left\lceil \frac{R_B^{(T)}}{97\hat{\nu}[n+1]} \left( \frac{(N_F - N_1)(97\hat{\nu}[n+1]+65)}{2N_2} - 65 \right) \right\rceil. \quad (4)$$

After obtaining $R_B[n+1]$, there still remains the problem of how to distribute these $R_B[n+1]$ RBs among the active video and data calls so that the reduction in overall QoE is minimized. To solve this problem, we first study the definition of cost functions that relate the reduction in QoE to the number of assigned RBs for video and data traffic. One challenge associated with the distribution of a budget of RBs between video and data calls is the dissimilar nature of the two traffic types. This challenge is certainly not new and there exists multiple solutions that could be adopted. Notwithstanding other options, we present next a solution inspired on our earlier work to schedule voice and data traffic [25].

As said earlier, the QoE for video traffic is measured through the PSNR and for data traffic is measured through the relative average delay increase. Without loss of generality, in order to match the QoE reduction for video and data users we assume that a 1 dB decrease in video PSNR corresponds to a 10% relative increase in data average delay (and a 3 dB decrease in PSNR corresponds to a 30% relative increase in average delay, etc.). Since the function for video PSNR versus bit rate (equivalent to RBs assigned) changes with the characteristics of the video sequence itself, we combine the PSNR-bit rate functions for multiple video sequences into one average PSNR-bit rate curve. The video sequences used were a mix of MPEG-4 coded video sequences at different resolutions, 240p, 360p and 480p, that were combined in the respective proportions 39%, 32% and 28% because these were the proportion for video request of different resolutios reported in [28]. The video sequences used were "Flowervase" and "Race Horses", at 30 frames per second (fps) for resolution 240p and 480p, and "Tennis" and "Park Scene", at 24 fps for resolution 360p. As a result, it was observed that the combined PSNR-bit rate curve can be very closely approximated with a function of the form $q_V = a \log r + b$, where $q_V$ is the video quality measured in PSNR, $r$ is the bit rate and $a$ and $b$ are constants. Setting the best video quality at almost $q_V^{(M)} = 38$ dB (achievable with a bit rate of 2 Mbps), a quality decrease cost function for video can be defined as $C_V = (q_V^{(M)} - q_V(r))/10$, where the factor 10 is introduced to make a 1 dB quality reduction equal to a value of 0.1. After replacing constants and operating, $C_V = -1.04 \log(R_B^{(V)}/R_B^{(T)})$, where $R_B^{(V)}$ is the number of RBs allocated to video.

The cost function for data traffic is calculated based on the relative increase in average delay. The data average delay can be modeled using Little's formula for an assumed M/D/1 queue, [26]:

$$Q = \frac{1}{2\mu} \left( \frac{2-\rho}{1-\rho} \right), \quad (5)$$

where $Q$ is the delay, $\mu$ is the service rate (in bps for this case and depending on the SINR and number of average RBs allocated), $\rho = \lambda/\mu$ is the traffic intensity and $\lambda$ is the average arrival rate (also in bps) to an eNB when traffic arrives following a Poisson model. When data traffic is shaped, the average delay becomes,

$$Q_S = \frac{1}{2\mu\pi_D[n]} \left( \frac{2\pi_D[n]-\rho}{\pi_D[n]-\rho} \right), \quad (6)$$

where $\pi_D[n] = R_B^{(D)}/R_B^{(T)}$ and $R_B^{(D)}$ is the number of RBs allocated to data. Note that this relation establishes a lower limit on $\pi_D[n]$, since for the queue to be stable $1 \geq \pi_D[n] > \rho$. Using (5) and (6), the relative increase in delay $Q_S/Q$ equals,

$$\frac{Q_S}{Q} = \frac{(1-\rho)(2\pi_D[n]-\rho)}{\pi_D[n](2-\rho)(\pi_D[n]-\rho)}, \quad (7)$$

and the cost function for data traffic is defined as $C_D = Q_S/Q - 1$, which is a function of the RBs assigned and the traffic intensity $\rho$.

From the cost functions $C_V(i)$ for video call $i$ and $C_D(j)$ for data session $j$, the overall cost function is defined as $C = \sum_i C_V(i) + \sum_j C_D(j)$, where the first sum is over the set of all video calls and the second over all data sessions. The problem now becomes to allocate the budget of $R_B[n+1]$ RBs among the video and data calls so that the cost function $C$ (representing the decrease in QoE) is minimized. Since the cost functions $C_V(i)$ and $C_D(j)$, while in principle different from each other, are both monotonically decreasing with the number of RBs assigned to the respective call, the problem is analogous to the problem of allocating a budget of time slots in

a TDMA frame to a set of voice calls, each in a different class with a different distortion-rate performance, so that overall distortion is minimized. In our case, each video or data call plays the role of a voice call, each of our cost functions plays the role of the distortion-rate function, the budget of RBs plays the role of the budget of time slots and our overall cost function plays the role of overall distortion. The analogous problem was optimally solved in [27] with the introduction of the greedy but optimal SEAMA algorithm. The algorithm is based on a table containing sorted entries for decremented costs. Let $\delta_i^{(j)} = C_j(i) - C_j(i+1)$ be the decremented cost for call $j$, when the number of assigned RBs is incremented from $i$ to $i+1$. An entry for call $j$ in a row number smaller than the row number for an entry for call $i$ needs to satisfy $\delta_j^{(k)} > \delta_i^{(l)}$ (decremented costs are stored in decreasing order) and the entry for a decremented cost $\delta_j^{(i)}$ needs to be at a smaller row number than an entry for decremented cost $\delta_k^{(i)}$ for $j < k$ (RBs are allocated incrementally). The table entries actually stores the index $j$ for the call with decremented cost $\delta_i^{(j)}$ that corresponds with the sorted order described. Before building the table, a minimum number of RBs (set based on minimum QoE limits) is assigned to each call. After this assignment, the total budget of RBs to be allocated to a value $R_B^{(b)}$ equal to the initial budget $R_B^{(T)}$ minus the RBs initially allocated. Since each row entry in the table corresponds to the allocation of one RB from the budget, once the table is built, a number of RBs $R_B(j)$ is assigned to call $j$ which has $R_B(j)$ row entries in the sub-table from row 1 to row $R_B^{(b)}$. Proof of optimality and further discussion for this algorithm can be found in [27].

## IV. Simulation Results

We evaluated the presented technique through simulations that we implemented using the LTE simulator from TU Wien, [24]. The LTE network was configured as described in Sect. II. For the first set of results, each cell site was assumed to be equipped with a battery bank with a capacity capable of powering the eNB for 6 hours at an 80% load (the average load is actually 60% as per Fig. 1). With the assumption $T = 1$ hour, $M$ was taken equal to 6 to encompass the battery bank capacity. Also, each cell site was equipped with a 10 kW wind turbine and 12 MX Solar USA Suncase MX60-240 solar panels, placed facing south at 43° Lat. N. (Rochester, NY), with no shading from obstacles. The 12 panels occupy an area of 20.4 m$^2$. The study used actual wind and solar data collected for 100 days between May and August of 2013. The power output for the 10 kW wind turbine was obtained by scaling the measurements from a Fuhrlander FL 250 (with a 250 kW maximum power) turbine installed to partially power a plastic molding company near Rochester, NY. In doing so, it was considered that the larger 250 kW and the smaller 10 kW turbines had approximately the same efficiency. Because the 250 kW turbine is twelve years older, the progress in technology over this time makes reasonable that both turbines have approximately the same efficiency.

We based the model for the traffic being serviced at the eNB on [22], where a good model for 2015 in a mobile network is

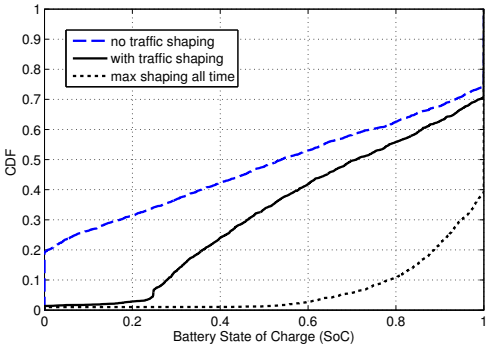


Fig. 4. Cumulative distribution functions (CDFs) for the battery SoC, $S[n]/B$, under different operating settings

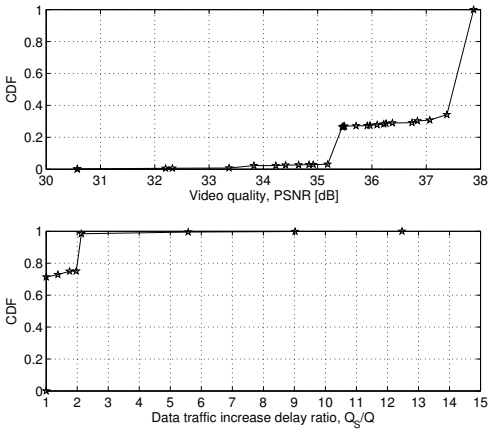


Fig. 5. The CDFs for the video quality (top) and for the relative increase in data traffic delay , $Q_S/Q$, with traffic shaping.

described as consisting of 20% of heavy users, which consume 2/3 of the radio resources. We combined this information with the data in [28], describing video requests in mobile networks being divided 39%, 32% and 28% between resolutions 240p, 360p and 480p, respectively. To evaluate the impact of traffic shaping on real-time video, its quality was calculated for the mix of video sequences described in Section III. Assuming a target video quality with peak signal-to-noise ratio (PSNR) almost 38 dB, the corresponding video traffic at a rate of 2 Mbps can be serviced in the simulated LTE network with two transmit antennas by allocating 10 RBs per frame (2/3 of the available RBs), 85% of the time. The target video rate of 2 Mbps and the allocation of 10 RBs agrees with the heavy user model in [22]. For data traffic, it was assumed that in each frame two users received service at a rate 200 kbps. In the simulated LTE system, each data user is serviced by allocating 2 RBs per frame 80% of the time. The combine traffic of an average 3 active users per frame and sector agrees with the average 9 users per eNB and frame reported in [22].

Figures 4 and 5 show results when the threshold for battery deep discharge was set at $L = 0.25$. Figure 4 shows the performance of the proposed technique evaluated by measuring the cumulative distribution (CDF) for the battery bank SoC, $S[n]/B$ compared to a system that implements maximum traffic shaping (transmission with only one antenna on all sectors all the time) and to a system that does not implement any traffic shaping technique. Fig. 4 shows that when

implementing traffic shaping all the time, the eNB operates powered from renewable sources of energy and the battery maintains a charge above the threshold of 25%, 99% of the time. Yet, implementing traffic shaping all the time implies that the users' QoE is reduced to its minimum acceptable value permanently, a setup that does not meet the goals for our design. On the other extreme, the eNB with no traffic shaping cannot be powered from renewable energy 20% of the time approximately, and the batteries operate into a deep discharge cycle 34% of the time. With the proposed traffic shaping technique the probability that the batteries operate in a deep cycle is reduced to 5%, approximately, and a probability of operating from renewable sources equal to 98.5%.

The results in Figure 4 clearly shows how the proposed scheme improves the operation from renewable energy, reducing the probability of not being able to power from renewable energy more than ten times and the probability of operating the battery bank into a deep discharge cycle almost seven times (this would result in extending the lifetime of the battery bank approximately by the same factor). At the same time, the improvements with the proposed scheme result from implementing a shaping of the cellular traffic that presents a tradeoff with the users' QoE. Figure 5 shows results that evaluate the performance for this second side of the tradeoff. At the top of figure 5 we show the cumulative distribution function (CDF) for the real-time video traffic (measured in PSNR) obtained during the duration of the simulation run. The figure shows that the renewable energy performance in the proposed scheme is obtained by reducing video quality in only one third of the time, approximately. Even more, when the video quality is reduced, approximately 98% of the time the quality is kept within a very acceptable and slightly noticeable 3 dB of the best quality value. Also, the video quality is reduced by more than 4 dB only 0.7% of the time and is never less than 30.5 dB which ensures always maintaining minimum acceptable QoE levels. At the bottom of figure 5 we show the cumulative distribution function (CDF) for the relative increase in data traffic average delay, $Q_S/Q$, obtained during the duration of the simulation run. The results show that data traffic average delay is increased only 29% of the time and less than 2% of the time the average delay is approximately more than doubled. The results also show a few corner cases (probability of occurrence less than 0.5%) of large relative increase in data traffic average delay (more than five times) that are attributed to users that were at locations within the eNB coverage area with very degraded wireless link quality (during the setup design, the minimum guaranteed resource allocation were set so that the probability of these event was very low as observed in the results).

Finally, we set to compare in figures 6 and 7 the proposed traffic shaping technique with the one we presented in [17]. While in a simplified view the two techniques differ in that the work in [17] does traffic shaping only on RBs and the proposed technique in this paper does traffic shaping on RBs and number of transmit antennas, vis-a-vis comparison between the two techniques is not as straightforward as the simplified view

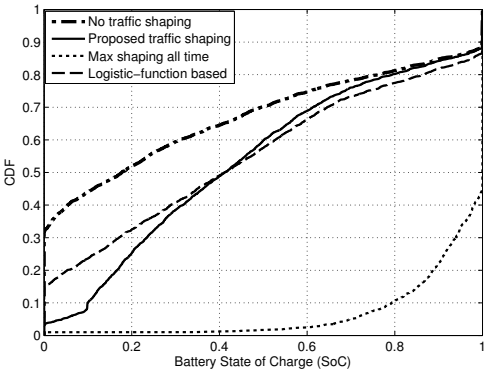


Fig. 6. Comparison of the cumulative distribution function (CDFs) for the battery SoC, $S[n]/B$ of the proposed technique with the technique presented in [17] ("Logistic-function based").

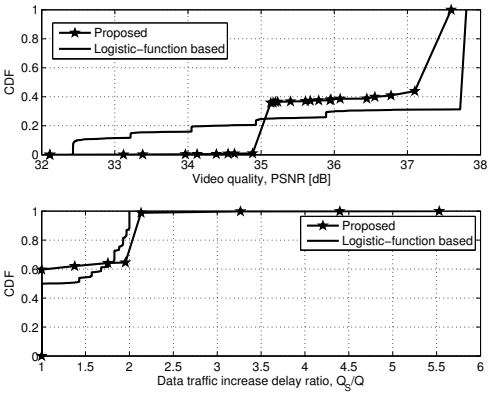


Fig. 7. Comparison of the CDFs for the video quality (top) and for the relative increase in data traffic delay , $Q_S/Q$, with traffic shaping, of the proposed technique with the technique presented in [17] ("Logistic-function based").

may imply because the techniques also differ in the goal set for the battery bank operation. Because of this, comparison with [17] required relaxing the goal for the proposed traffic shaping technique and setting the deep discharge threshold at a very low level of $L = 0.1$. Other settings for this simulation (equal to those in [17]) were a wind and solar generators setup consisting of a 10 kW wind turbine and 6 MX Solar USA Suncase MX60-240 solar panels. The battery bank was assumed with a capacity capable of powering the eNB for 8 hours at an 80% load and $M = 8$. In the figures 6 and 7, the results from [17] were labeled as "Logistic-function based" because of the function used to determine the target battery level $S_T[n + 1]$. While, as discussed, a study of battery operation within the deep discharge regime is not applicable in this case, figure 6 shows that the traffic shaping technique presented herein achieves a much lower percentage of time (3.5% versus 15%) when the eNB is not powered from renewable energy. At the same time, figure 7 shows that the proposed traffic shaping technique has a much better performance in terms of reduction of the users' QoE than the technique in [17] (if we accept that a relative increase in data average delay of 2 and 2.1 are essentially the same). Overall, the results in figures 6 and 7 validate the three remarks made in Section III.

## V. Conclusions

In this paper we have presented an integrated energy-traffic management technique for sustainable LTE cellular networks where cell sites are powered most of the time from renewable energy generators. Based on the renewable energy projected deficit or surplus, the proposed technique achieves a more sustainable operation by shaping the traffic at the cellular base stations to increase and make a more effective use of renewable energy, while having a reduced effect on real-time traffic (video) quality and average data delay. This approach is novel in that it treats traffic conditions and QoE requirements as controllable parameters. The real time video traffic can be controlled without adding any delay by leveraging the scalability features found in modern video codecs and the data traffic is controlled by adapting the transmit throughput. In the proposed technique, power consumption at the eNB is reduced by shaping traffic through the control of the number of active transmit antennas and resource blocks. The evaluation results, based on 100 days of wind and solar power measurements, show that with the presented technique an LTE eNB can be powered from renewable energy 95% of the time while avoiding operating the battery bank in a lifetime-reducing deep discharge cycle. The proposed technique reduces the probability of not being able to power the base station from renewable energy more than ten times (from 20% to 1.5%) and reduces seven times the probability of operating the battery bank into a deep discharge cycle. More importantly, these results are achieved while introducing minor effects on the real-time and data traffic. Indeed, with the presented technique, video and data traffic are affected less than a third of the time, video quality is reduced by more than 3 dB only 2% of the time and data delay is approximately more than doubled only 2% of the time.

## References


[1] Webb, M.; "Smart 2020: Enabling the Low Carbon Economy in the Information Age", *The Climate Group Tech. Report*, 2008.

[2] Bianzino, A.P.; Chaudet, C.; Rossi, D.; Rougier, J., "A Survey of Green Networking Research", *IEEE Communications Surveys and Tutorials*, vol.14, no.1, pp.3-20, 2012.

[3] Vadgama, S.; Hunukumbure, M.; "Trends in Green Wireless Access Networks", *IEEE International Conference on Communications Workshops (ICC)*, June 2011.

[4] Xiaofei Wang; Vasilakos, A. V.; Min Chen; Yunhao Liu; Ted Taekyoung Kwon; "A Survey of Green Mobile Networks: Opportunities and Challenges", *Journal Mobile Networks and Applications* vol. 17, No. 1, Feb. 2012.

[5] Altman, E; Hanawal, M. K.; ElAzouzi, R.; Shamai, S.; "Tradeoffs in green cellular networks", *SIGMETRICS Perform. Eval.*, Rev. 39, 3 (December 2011), 67-71.

[6] Zhisheng Niu; Yiqun Wu; Jie Gong; Zexi Yang;; "Cell zooming for cost-efficient green cellular networks", *IEEE Communications Magazine*, vol.48, no.11, pp.74-79, November 2010.

[7] Herlich, M.; and Karl, K.; "Reducing power consumption of mobile access networks with cooperation", *2nd Int. Conf. on Energy-Efficient Comp. and Net. (e-Energy '11)*, pp. 77-86, 2011.

[8] Jin, J.; and Li, B; "Cooperative resource management in cognitive wimax with femto cells," *IEEE INFOCOM*, pp. 19, March 2010.

[9] Phuyal, U.; Jha, S.C.; Bhargava, V.K., "Green resource allocation with QoS provisioning for cooperative cellular network", *12th Canadian Workshop on Inf. Theory (CWIT)*, pp.206-210, 2011.

[10] Videv, S.; Thompson, J. S.; Haas, H.; Grant, P. M., "Resource allocation for energy efficient cellular systems", *EURASIP Journal on Wireless Comm. and Net.*, vol. 2012, no. 1, pp. 1-15.

[11] Congzheng Han; Armour, S., "Adaptive Power and Resource Allocation Strategies for Green Radio", *IEEE Global Telecommunications Conference (GLOBECOM)*, pp.1-5, 2011.

[12] Jie Gong; Sheng Zhou; Zhisheng Niu, "Optimal Power Allocation for Energy Harvesting and Power Grid Coexisting Wireless Communication Systems", *IEEE Transactions on Communications* vol.61, no.7, pp.3040-3049, 2013.

[13] Marsan, M.A.; Bucalo, G.; Di Caro, A.; Meo, M.; Yi Zhang, "Towards zero grid electricity networking: Powering BSs with renewable energy sources", *IEEE International Conference on Communications Workshops (ICC)*, pp.59-601, 2013.

[14] Chia, Yeow-Khiang; Sun, Sumei; Zhang, Rui, "Energy cooperation in cellular networks with renewable powered base stations", *IEEE Wireless Communications and Networking Conference (WCNC)*, pp.2542-2547, 2013.

[15] Gong, Jie; Thompson, J. S.; Sheng Zhou; Zhisheng Niu; "Base Station Sleeping and Resource Allocation in Renewable Energy Powered Cellular Networks", *arXiv preprint*: 1305.4996, 2013.

[16] Kwasinski, A.; Kwasinski, A.; "Architecture for green mobile network powered from renewable energy in microgrid configuration", *Wireless Communications and Networking Conference (WCNC)*, pp. 1273-1278, 2013.

[17] Kwasinski, A.; Kwasinski, A.; "Traffic Management for Sustainable LTE Networks", *IEEE Global Telecommunications Conference (IEEE GLOBECOM)*, pp. 2520-2525, December 2014.

[18] Zhoujia Mao; Koksal, C.E.; Shroff, N.B., "Resource Allocation in Sensor Networks with Renewable Energy", *Proceedings of 19th International Conference on Computer Communications and Networks (ICCCN)*, pp.1-6, 2-5,2010.

[19] Tutuncuoglu, K.; Yener, A., "Optimum Transmission Policies for Battery Limited Energy Harvesting Nodes", *IEEE Trans. on Wireless Communications*, vol.11, no.3, pp. 1180-1189, 2012.

[20] Kwasinski, A.; Krishnamurthy, V.; Song, J.; Sharma, R.; "Availability Evaluation of Micro-Grids for Resistant Power Supply During Natural Disasters", *IEEE Transactions on Smart Grid*, vol.3, no.4, pp.2007-2018, Dec. 2012.

[21] Kwasinski, A.; Krein, P. T.; "Stabilization of Constant Power Loads in DC-DC Converters Using Passivity-Based Control", *2007 Int. Telecom. Energy Conf. (INTELEC)*, pp. 867-874.

[22] Auer, G.; Blume, O.; Giannini, V.; Gdor, I.; Imran, M.; et al.; "Energy Efficiency Analysis of the Reference Systems, Areas of Improvements and Target Breakdown", *Energy Aware Radio and neTwork tecHnologies (EARTH) Project deliverable D2.3*, document INFSO-ICT-247733 EARTH, (2010).

[23] Rec. ITU-R M.1225, *Guidelines for evaluation of radio transmission technologies for IMT-2000*, 1997.

[24] Ikuno, J. C.; Wrulich, M.; Rupp, M.; "System level simulation of LTE networks", *in Proc. 2010 IEEE 71st Vehicular Technology Conference*, Taipei, Taiwan, May 2010.

[25] Kwasinski, A.; Alasti, M.; Liu, K. J. R.; Farvardin, N.; "A Low Complexity Source Encoding Assisted Multiple Access Protocol for Voice/Data Integrated Networks", EURASIP Journal on Applied Signal Processing, vol. 2005, issue 2, pp. 193-206, 2005.

[26] W. Stallings, "High-Speed Networks TCP/IP and ATM Design Principles", Prentice Hall, 1998.

[27] M. Alasti and N. Farvardin, "SEAMA: a source encoding assisted multiple access protocol for wireless communications", *IEEE Journal on Selected Areas in Communications*, vol. 18, no. 9, pp. 16821700, 2000.

[28] Byte Mobile, *Mobile Analytics Report*, June 2011.